Conceptual Design of a Mars-Oriented Blended Wing Body Aircraft with Distributed Propulsion

Sohini Gupta[1]
Wheeler High School, Marietta, Georgia, 30068, USA

Adeel Khalid[2]
Kennesaw State University, Marietta, Georgia, 30060, USA

The present paper describes the design and development of three different Blended Wing Body (BWB) Aircrafts with Distributed Propulsion for the mission of being deployed in the Mars atmosphere. This set of aircraft are the Martian Aerial Reconnaissance Vehicle for Intraplanetary Navigation (MARVIN) models. These design concepts are tailored for payload flight containing instruments for the purpose of environmental survey. The three different aircrafts designed in this study are for three different weight classes: less than 500 lbs, 500-5000 lbs, and 5000-50,000 lbs. These aircrafts must follow a set of requirements to be able to conduct environmental surveys and for survivability on Mars. Details of this paper include mission profiles, concept sketch iterations, empty weight and fuel fraction estimations, takeoff weight calculations, as well as CAD models of the aircraft and CFD analyses. Comparative CFD analyses determine the lift and drag values for each aircraft, help evaluate the velocity and pressure plots, validate various dimensions, and compares BWB to traditional aircraft.

I. Nomenclature

Fx	=	*X* component of the force; drag
Fz	=	*Z* component of the force; lift
N	=	Newtons
kg	=	kilograms
lbs	=	pounds
m	=	meters
ft	=	feet
m/s	=	meters per second
mph	=	miles per hour
BWB	=	Blended Wing Body
Re	=	Reynolds Number
R	=	range
TSFC	=	Thrust Specific Fuel Consumption
C	=	TSFC at aerodynamic design point
V	=	velocity
L/D	=	lift-to-drag ratio
E	=	endurance

[1] High School Student, AIAA High School Member
[2] Professor, Industrial & Systems Engineering, and AIAA Life Member Grade

II. Introduction

Blended Wing Body (BWB) aircrafts are a type of aircraft characterized by the seamless integration of wings into a fuselage, or body, in order to create an optimal aerodynamic shape for a higher lift-to-drag ratio. The concept first emerged in the mid-20th century, when there was a need for improved fuel efficiency as well as reduced drag. Various prototypes and experimental models, such as the Boeing X-48 series, have provided proof and demonstration of its aerodynamic and efficiency advantages and contributions to ongoing research in both commercial and military aircraft. The use of distributed propulsion in aircraft has provided additional safety through the redundancy of using multiple engines and reduction in noise [7]. The aim of the proposed conceptual design is to produce aircrafts that incorporate both a blended wing body and distributed propulsion and can carry a certain amount of payload, such as instruments, and/or crew in three different weight classes: below 500 lbs, 500-5000 lbs, and 5000-50,000 lbs. Moreover, the specified use would be for the Martian atmosphere, considering factors that allow for longevity and survivability on the planet. This provides new research avenues for optimized Martian aircraft, propelling research towards both advanced surveying methods of Mars and commercialized aircraft on an extraterrestrial planet. The general process for this aircraft design includes collecting historical data on the characteristics of blended wing body aircraft, such as empty weight and gross weight, calculating estimations of empty weight and takeoff weight as well as fuel fraction based off of early concept sketch iterations, selecting airfoil and aircraft geometry, creating a digital 3D model in a CAD software, and performing fluid analysis [20].

Investigators have been putting in immense efforts into the research and development of the Blended Wing Body (BWB) aircraft for its numerous advantages in optimizing aviation in terms of aerodynamic characteristics. Fuel has become the leading contribution to an increase in cost for airliners; unconventional aircraft such as BWBs could be a solution to significantly reduce emissions as well as noise, therefore reducing the cost [10]. As a byproduct, this would create an outline for greener airlines. BWBs create the opportunity to have aircraft with enhanced and longer-range performance through the increase of the lift-to-drag ratio [10]. In other words, compared to traditional tube-and-wing aircraft, the BWB has a higher-level aerodynamic performance.

Although research for Martian aircraft is not relatively new, there are a limited number of designs that have been proposed. Moreover, in the topic of a fixed wing aircraft for Mars, which is even more narrow, no designs have been built, tested, and used for the actual environment of Mars. Mars has been explored by rovers and satellites, but only one rotary-wing aircraft. The number of aircraft that can be referred to for this specific use is very few.

Because of Mars' environmental aspects, designing a Martian aircraft becomes extremely difficult. The biggest challenge comes from the low atmospheric density of Mars [3]. Considering how thin the Martian atmosphere is, conventional aircraft would have to travel at extremely high speeds, making take-off and landing maneuvers nearly impossible for more cruise flights than one [4]. Propulsion systems must rely on either chemical or electrical systems because of how low the oxygen content is [4]. Out of the aircraft that can be referred to as a starting point in this design process of the BWB, the bulk of conventional aircraft is out of the question.

III. Literature Review

Withrow-Maser et al. discusses conceptual designs of advanced rotorcraft designs. These designs are larger in scale compared to the Ingenuity, and use non-traditional airfoils to enhance performance [1]. Mishra et al. presents the design process for a conceptual Unmanned Aerial Vehicle for the Martian atmosphere. Its capabilities include vertical take-off and landing and carrying payload equivalent to 5kg on Mars [2]. Fujita et al. proposes the conceptual design of a fixed-wing Mars Airplane that could be packed into an aeroshell. The packing allows for the wing area to be maximized. It considers the many constraints that are set by the Martian environment [3]. Walker conducts aerodynamic, stability, and control evaluations of a newly proposed Mars airplane design that is rocket-powered called the Argo VII. Its range is 373 km as shown through the evaluation and can adequately provide a means of collecting scientific data on Mars [4].

Kim describes early concepts of distributed propulsion vehicles as well as current turboelectric distributed propulsion vehicles that are being studied under NASA's Subsonic Fixed Wing Project. Many concepts are based on distributed jet flaps, small multiple engines, gas-driven multi-fans, etc. [5]. Felder et al. analyzes the performance of a 300-passenger hybrid wing body with turboelectric distributed propulsion called the N3-X. The purpose is to determine whether the aircraft meets the 70% fuel burn reduction goal of NASA's Subsonic Fixed Wing Project [6]. Leifsson et al. consider a distributed propulsion concept for aircraft, involving replacing a small number of large engines with a larger number of small engines. A blended wing body was used to test the distributed propulsion concept [7]. Felder et al. presents a propulsion system that transmits power from a turbine to a fan electrically. The ease of electric distributions opens up many new possibilities for aircraft propulsion, which are all discussed [8]. Kim

et al. performs study of the electric power distribution system in the N3-X, a hybrid wing body aircraft that uses a turboelectric propulsion system. The different features and issues associated with the system are reviewed [9].

Lyu and Martins perform a series of studies to optimize the shape of Blended Wing Body aircraft. In these studies, 273 different design variables such as twist, airfoil shape, and span are considered [10]. Brown and Vos present a conceptual design of a Blending Wing Body aircraft and perform comparisons with Tube and Wing aircraft. Each type of aircraft was created and tested for 150, 250, and 400 passenger classes [11]. Humphreys-Jennings et al. performs a study aimed to design a Blended Wing Body aircraft and test its flying and handling qualities. The proposed aircraft has a range of 3000 nautical miles and can carry 200 passengers [12]. Dorsey and Urange design and optimize a Blended Wing Body (BWB) aircraft and compare its performance with the conventional tube and wing aircraft. Design considerations include single deck and double deck passenger layouts. BWBs perform best for long range missions with more than 200 passengers [13]. Qin et al. studies the effects of spanwise lift distribution on the aerodynamic efficiency of a Blended Wing Body (BWB) aircraft. The baseline BWB model is modified for elliptical and triangular spanwise loading distribution, and then analyzed [14].

Désert et al. develops a propulsion system for a rotary wing vehicle with the purpose of Mars exploration. The impact of airfoil optimization and vortex production are estimated; airfoils delaying heavy unsteadiness generation produce higher lift and lower drag [15]. Hidaka and Okamoto study different triangular-shaped airfoils in wind tunnel tests conducted at low Reynolds number ranges. The purpose is to clarify aerodynamic characteristics in a simulated Mars atmosphere [16]. Oyama and Fujii develop an optimal airfoil design for future missions that implement the usage of a Mars airplane. The design is compared with existing airfoils that were optimized at either a different Reynolds number or a different Mach number. The effects of the differences on the design are discussed [17]. Rajarajan et al. implements a study of fluid dynamics on different airfoils based on the conditions of the Mars atmosphere. The types of airfoils tests include Ishii, Profiled Dragonfly, and Triangular. These were imported into an ANSYS Fluent for the Numerical simulation [18]. Șugar-Gabor and Koreanschi present optimized airfoil designs in both single-point and multi-point. The airfoils were designed for high-subsonic low Reynolds number flow regime, specifically the Martian atmosphere. Both fully turbulent and transitional flow are considered [19].

Raymer provides a comprehensive framework for the design process of an aircraft. This step-by-step instruction can be used as a basis for each stage of aircraft design, and includes historical data as needed for certain calculations [20].

IV. Methodology

The set of aircraft models developed in this study are called the MARVIN models, where MARVIN stands for Martian Aerial Reconnaissance Vehicle for Intraplanetary Navigation. MARVIN500 is the model in the <500 lbs maximum takeoff weight range, MARVIN5K corresponds to 500-5000 lbs, and MARVIN50K corresponds to 5000-50000 lbs.

In this section, the process through which each MARVIN model was conceived and designed is discussed. The criteria, constraints, and goals are explained thoroughly and broken down into different parts.

A. Mission Profile

The requirements which each MARVIN aircraft must follow are carefully depicted in each mission profile to accomplish the aircrafts' survivability and longevity in the Martian atmosphere.

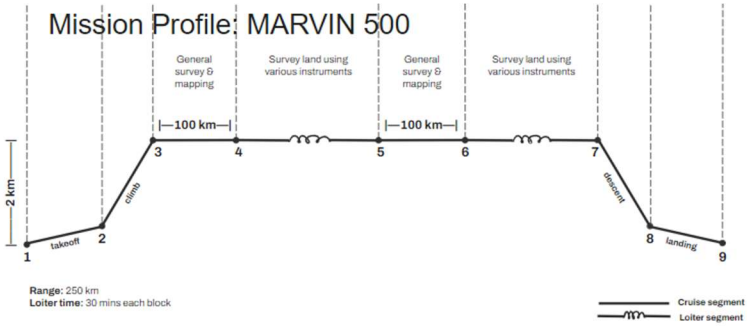

(a)

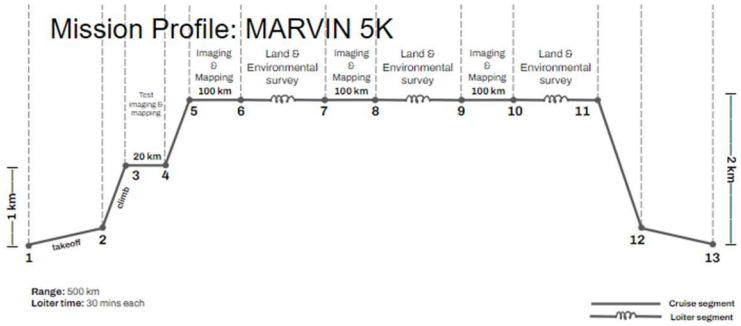

(b)

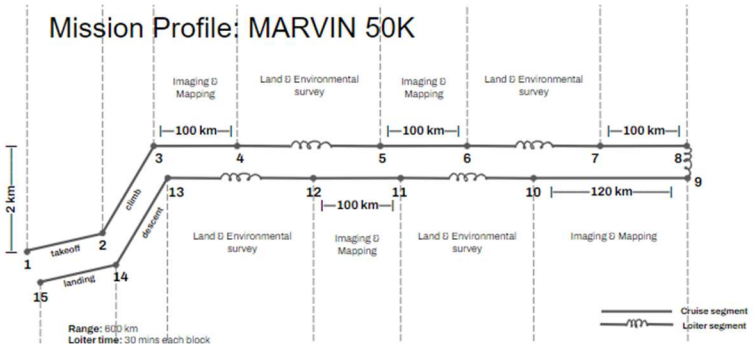

(c)

Fig. 1 a) MARVIN500 Mission Profile, b) MARVIN5K Mission Profile, c) MARVIN50K Mission Profile

B. Reynolds Number Calculations

The Reynolds Number (Re) is a dimensionless value that characterizes the flow of a fluid around an object. This value is calculated using the cruise speed, airfoil chord length, and kinematic viscosity of the atmosphere.

1. Cruise Speed Estimation

The cruise speed estimation for each MARVIN model is determined by finding the cruise speeds of BWB models in the same weight class and averaging the values (Table 1). *Due to limited data on BWB aircraft, the data for general fixed-wing UAVs are used. **Some of these UAV models incorporate BWB concepts.

Table 1 Cruise Speed Estimations

<500lbs Models	**Cruise Speed (mph)**	**500-5000 lbs Models**	**Cruise Speed (mph)**	**5000-50000 lbs Models**	**Cruise Speed (mph)**
Boeing X-48	104	**Miles M.30	350	**McDonnel XP-67	270
Northrop Grumman Bat	69	*MQ-1	90	Boeing X-45A	613
ARES-2	130	*MQ-9a	194	Northrup Grumman X-47b	690
Argo VII	324	*Elbit Hermes 900	70	**CBY-3	193
*Boeing Insitu MQ-27 ScanEagle	69	-	-	-	-
Average Speed (mph)	139.2	**Average Speed (mph)**	176	**Average Speed (mph)**	441.5
Average Speed (m/s)	62.23	**Average Speed (m/s)**	78.68	**Average Speed (m/s)**	197.37

2. Airfoil Chord Estimation

The airfoil chord estimation for each MARVIN model is found by averaging the root chord length and tip chord length values (Table 2). Both of these values are determined in conceptual sketches.

Table 2 Airfoil Chord Estimations

	MARVIN500	MARVIN5K	MARVIN50K
Root Chord Length (ft)	9	21	10
Tip Chord Length (ft)	3	9	40
Average Chord Length (ft)	6	15	25
Average Chord Length (m)	1.83	4.57	7.62

3. Reynolds Number Estimation

The Reynolds number is calculated using the equation vl/μ (Eq. 1), where v is the speed of the aircraft, found from the average speed calculations in Table 1, l is the characteristic length which is the average chord length of the airfoil and is equal to the average width of the wing, and μ is the kinematic viscosity of the Martian atmosphere. This value is calculated for each of the MARVIN models (Table 3).

The Kinematic Viscosity of the Martian Atmosphere, which is a value being used in this estimation, is 0.000964 m/s^2.

Table 3 Reynolds Number Estimation

Model	Reynolds Number (Re)
MARVIN500	118,052.39
MARVIN5K	373,154.11
MARVIN50K	1,560,109.32

C. Empty Weight Calculations

For each weight class, the empty weight to gross weight ratio, also known as the empty weight ratio, was calculated by averaging the empty weight ratios for known Blended Wing Body models in that weight category (Table 4, Table 5, Table 6). If not enough data points are found, data for known unmanned fixed-wing aircraft in that weight category is used instead.

Table 4 Historical Data for Empty Weight Ratios: <500 lbs

Model	Empty Weight (lbs)	Gross Weight (lbs)	Empty/Gross
Argo VII	246	362	0.680
Northrup Grumman Bat	275	350	0.786
ARES-2	280	386	0.725
Boeing X-48	392	500	0.784

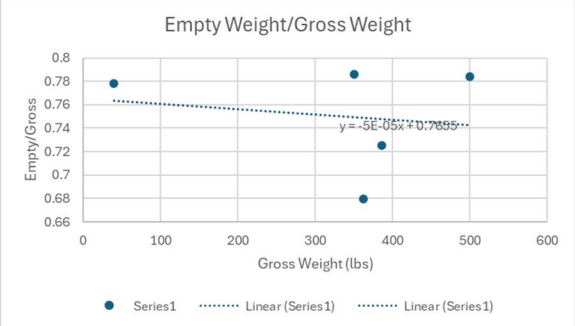

Fig. 2 Empty Weight Ratio Graph: <500 lbs

Table 5 Historical Data for Empty Weight Ratios: 500-5000 lbs

Model	Empty Weight (lbs)	Gross Weight (lbs)	Empty/Gross
**Miles M.30	2710	4240	0.639
*MQ-1 Predator	1130	2249	0.502
*MQ-9A Reaper	4901	10,494	0.467
*Elbit Hermes 900	970	1100	0.882

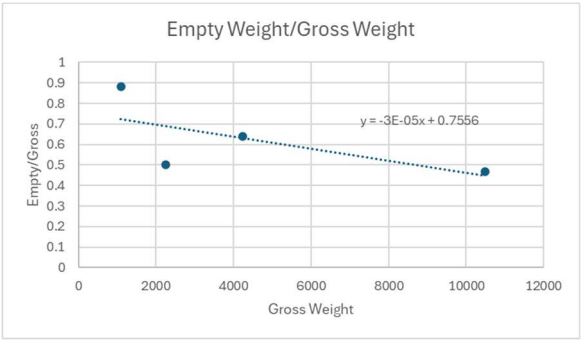

Fig. 3 Empty Weight Ratio Graph: 500-5000 lbs

Table 6 Historical Data for Empty Weight Ratios: 5000-50000 lbs

Model	Empty Weight (lbs)	Gross Weight (lbs)	Empty/Gross
Northrup Grumman x-47b	28,837	44,501	0.648
**McDonnel XP-67	17,745	22,114	0.802
**CBY-3	16,800	27,000	0.622
Boeing X-45A	8000	12,140	0.659

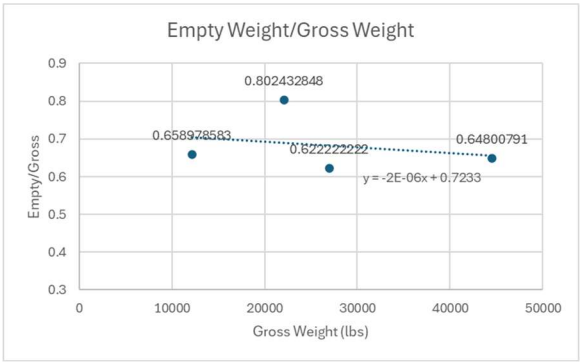

Fig. 4 Empty Weight Ratio Graph: 5000-50000 lbs

From the values in Table 4, Table 5, and Table 6, the best fit line in Figure 4, Figure 5, and Figure 6 are created. The average empty weight to gross weight ratio for MARVIN500 is determined to be 0.752, 0.582 for MARVIN5K, and 0.686 for MARVIN50K.

D. Fuel Fraction Calculations

Fuel fraction estimation is based on the mission to be flown found in mission profiles, approximations of fuel consumption, and approximations of aerodynamics (Raymer, 1992). The fuel fraction is equal to the final weight of the fuel after the mission completed divided by the initial weight of the fuel.

For warmup & takeoff, climb, and landing, the fuel fractions are generally constant through different mission profiles. To calculate the fuel fraction for cruise segments, the cruise distance (range), estimated L/D, estimated velocity, and TSFC are needed. To calculate the fuel fraction for loiter, the loiter time also known as the endurance, L/D estimation, and TSFC are needed.

1. Known Values for Flight Segment

The fuel fraction estimation for the warmup & takeoff, climb, and landing segments are generally known for initial sizing and recorded below in Table 7.

Table 7 Known Flight Segment Values [20]

Segment	Fuel Fraction
Warmup & Takeoff	0.97
Climb	0.985
Landing	0.995

The Thrust Specific Fuel Consumption (TSFC) is used in this study as a constant value to calculate the fuel fraction. For turboelectric distributed propulsion, this value is found to be 0.47 lbm/(lbf*hr) at the aerodynamic design point, or cruise [9]. For the cruise segment, the ceiling of this value is used (0.5), while for the loiter segment the floor of this value is used (0.4).

2. L/D Estimation

For an early estimation of L/D, the wetted-area ratio, which compares the aircraft's wingspan to the exposed surface area, can be used as a reliable relationship. In other words, the wetted-area ratio for a certain type of aircraft corresponds to an L/D estimate. These values for each of MARVIN models are recorded in Table 8.

Table 8 L/D Estimation [20]

Model	Max L/D Ratio	Wetted Area Ratio	Max L/D (Loiter)	Max L/D (Cruise)
MARVIN500	23	3	23	19.918
MARVIN5K	22	2.3	22	19.052
MARVIN50K	22.5	2.65	22.5	19.485

3. Cruise Fuel Fraction Estimation

The fuel fraction for the cruise section is equal to the weight of the fuel after the segment is completed divided by the weight of fuel before the segment is completed. The fuel fraction values for each MARVIN model are recorded in Table 9. The equation used for calculating this value is a rearranged Breguet range equation:

$$\frac{W_i}{W_{i-1}} = e^{\frac{-RC}{V(\frac{L}{D})}} \text{ (Eq. 2)}$$

Table 9 Cruise Fuel Fraction Estimations

	MARVIN500	MARVIN5K	MARVIN50K
Cruise Range 1 (km)	100	20	100
Cruise Range 1 (ft)	328,083.99	65,616.80	328,083.99
Cruise Range 2 (km)	-	100	120
Cruise Range 2 (ft)	-	328,083.99	393,700.79
L/D Estimation	19.918	19.052	19.485
Velocity (m/s)	62.23	78.68	197.37
Velocity (ft/s)	204.16	258.14	647.54
TSFC (per hr)	0.5	0.5	0.5
TSFC (per sec)	0.000139	0.000139	0.000139
Fuel Fraction (Cruise Range 1)	0.989	0.998	0.9964
Fuel Fraction (Cruise Range 2)	-	0.991	0.9957

MARVIN500 has one cruise range, while MARVIN5K and MARVIN50K both have two cruise ranges as seen in the mission profiles in Figure 1. As a result, there are two different fuel fractions each for MARVIN5K and MARVIN50K.

4. Loiter Fuel Fraction Estimation

The fuel fraction for the loiter section is equal to the weight of the fuel after the segment is completed divided by the weight of fuel before the segment is completed. The fuel fraction values for each MARVIN model are recorded in Table 10. The equation used for calculating this value is a rearranged endurance equation:

$$\frac{W_i}{W_{i-1}} = e^{\frac{-EC}{\left(\frac{L}{D}\right)}} \text{ (Eq. 3)}$$

Table 10 Loiter Fuel Fraction Estimations

	MARVIN500	MARVIN5K	MARVIN50K
Endurance (hr)	0.5	0.5	0.5
Endurance (sec)	1800	1800	1800
L/D Estimation	23	22	22.5
TSFC (per hr)	0.4	0.4	0.4
TSFC (per sec)	0.000111	0.000111	0.000111
Fuel Fraction	0.9900	0.9896	0.9898

5. Total Fuel Fraction Estimation

By multiplying all the fuel fractions from each segment together, the total mission weight fraction, W_x/W_0, can be calculated. The total fuel fraction values for each MARVIN model are recorded in Table 11. This value is then used to calculate the total fuel fraction as seen in the equation below:

$$\frac{W_f}{W_0} = 1.06\left(1 - \frac{W_x}{W_0}\right) \text{ (Eq. 4)}$$

Table 11 Total Fuel Fraction Estimation

Model	W_x/W_0	W_f/W_0
MARVIN500	0.911	0.0942
MARVIN5K	0.881	0.126
MARVIN50K	0.886	0.121

E. Airfoil Data Interpolation

Out of a vast amount of airfoil models explored, five models used in past BWB models are used as a baseline and then similar models to these base models are found to determine the airfoil with the highest L/D for each calculated Re. The base models used include Sd7037, NASA SC(2)-0518, CLARK-Y, NACA 0012-34, and Eppler E387. The models used that are similar to the base models include Sa7035, S3014-095-85, Eppler E174, NACA 6409, and S7075.

For each airfoil model found, the data for the max L/D is collected for 5 Reynolds numbers from an airfoil database. This data is then plotted and fit to a logarithmic function which is then used to calculate the exact max L/D for the calculated Re. The max L/D for each airfoil model is recorded in Table 12.

Table 12 Airfoil Data Interpolation

Re	Sd7037 Max L/D	NASA SC(2)-0518 Max L/D	CLARK-Y Max L/D	NACA 0012-34 Max L/D	Eppler E387 Max L/D	Sa7035 Max L/D	S3014-095-85 Max L/D	Eppler E174 Max L/D	NACA 6409 Max L/D	S7075 Max L/D
50,000	34.5	26	29.6	25.9	38.1	33.2	32.5	38.1	27.1	38.8
100,000	55.2	25.9	53	39.2	60.7	52.8	51.9	61.4	61.6	59.6
200,000	74.7	36.5	73.2	47.6	84.4	71.3	70.3	84.9	87.1	81.3
500,000	99.3	59.3	98.7	49.1	116.3	94.9	92.4	117.3	122.4	108
1,000,000	116	77.3	114.8	56.4	140.6	111.4	106.6	141.9	151	123

MARVIN500 **118052.39**	58.67	34.39	56.68	38.03	66.59	56.82	55.64	67.26	63.99	64.85
MARVIN5K **373154.12**	89.97	55.23	89.36	48.61	106.06	86.86	84.18	107.19	110.60	97.65
MARVIN50K **1560109.32**	128.88	81.11	129.99	61.75	155.13	124.19	119.65	156.83	168.54	138.42

From Table 12, the airfoil model with the highest L/D value for each MARVIN model is found; this airfoil model is then incorporated into the corresponding MARVIN model (Table 13).

Table 13 Airfoil Identification

	Highest L/D	Airfoil Model
MARVIN500	67.26	**E174**
MARVIN5K	110.60	**NACA6409**
MARVIN50K	168.54	**NACA6409**

F. CAD Models

Using the conceptual sketches and selected airfoil models, the CAD models for each MARVIN model could be created. This is done by importing respective airfoil models into the CAD file, assigning appropriate dimensions, and lofting between airfoils to create the overall structure. After the overall structure is created, control surfaces and winglets are added to the model.

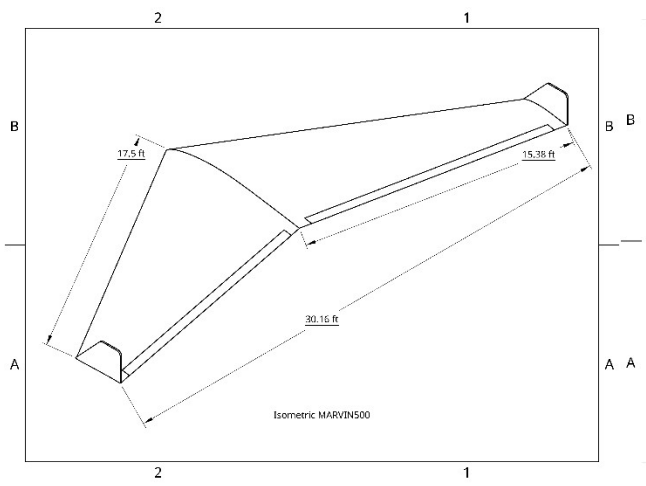

(a)

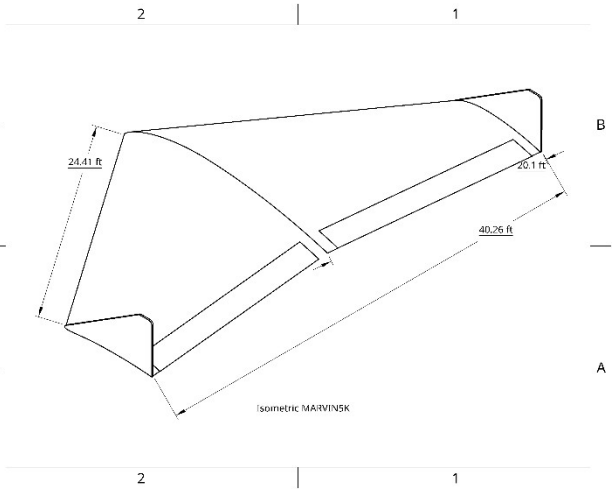

(b)

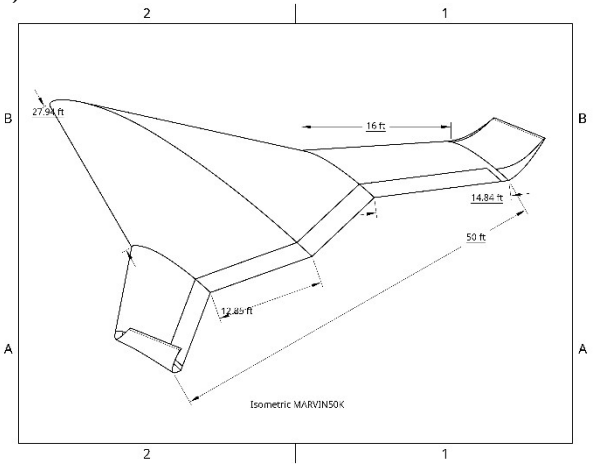

(c)

Fig. 5 (a) MARVIN500 CAD Drawing, (b) MARVIN5K CAD Drawing, (c) MARVIN50K CAD Drawing

G. CFD Simulations

Each aircraft used the same parameters other than the initial velocity, which is set as the corresponding average cruise speed. The parameters used include the type of air which is set to "Martian Atmosphere", gravity of Mars (3.73 m/s^2) in the negative z direction, altitude which is set to 2000m, and computational domain of the analysis where the width is four times the wingspan of the aircraft and the length is ten times the wingspan.

From the CFD analysis, the resulting force in the x-direction corresponds to drag, while the force in the z-direction corresponds to lift. The "Converged Lift" is the value of lift the simulation converged to and the "Average Lift" is the average calculated lift, both of which are similar values after several iterations of calculations. The same logic can be applied to "Converged Drag" and "Average Drag". To calculate L/D, the average lift is divided by the average drag (Table 14).

Table 14 Lift and Drag Values for MARVIN Models

Model	Converged Lift (N)	Average Lift (N)	Converged Drag (N)	Average Drag (N)	L/D
MARVIN500	4993.98	4994.24	399.78	399.87	12.49
MARVIN5K	28,896	28,907.7	3909.96	3916.09	7.38
MARVIN50K	501,441	500,712	48,280.3	48,276	10.37

1. Data Analysis

Using the L/D found in Table 14, whether the aircraft model could fly or not is determined by comparing the lift value (N) to the upper limit of the aircraft weight range on Mars (N). All three aircraft are designed to ensure that the lift is greater, so the aircraft can fly.

The upper limit of each weight range is converted from lbs to kg and then multiplied by 3.73, the value for acceleration of gravity generated by the gravitational field of Mars, to convert the value into Newtons. This value is then compared to the corresponding Average Lift from CFD Simulations. The upper limit is then subtracted from the Average Lift to determine the payload availability (Table 15).

Table 15 Payload Availability

Model	Average Lift (N)	Max Weight on Mars (N)	Payload Available (N)
MARVIN500	4994.24	764.30	4229.94
MARVIN5K	28,907.7	7643.03	21,263.97
MARVIN50K	500,712	76,430.31	424,281.69

"Payload" includes engines, avionics, electronics, fuel, and cargo/instruments; the lift is greater than the max weight on Mars for each MARVIN model, confirming that the aircraft will be able to fly.

V. Conclusion

This study proposes three aircraft designed to fly on Mars. These concepts could also be integrated into future Martian aircraft designs. There are, however, additional design considerations and analysis needed to complete a thorough evaluation and truly determine if the aircraft models are fit for use. This includes takeoff weight estimation, comparison to traditional aircraft, addition of configuration layout, wing-loading and thrust-to-weight calculations, and testing each aircraft at different angles of attack. The most accurate form of testing would be to create a physical model and conduct flight tests. Overall, in this study a high-level framework is created that can be utilized for consideration in future designs of Martian aircraft.

References

[1] Shannah Withrow-Maser et al., "An Advanced Mars Helicopter Design," Nasa.gov, Nov. 16, 2020. https://ntrs.nasa.gov/citations/20205008553 (accessed Nov. 21, 2024).

[2] I. Mishra, A. Kumar, and V. Malhotra, “Conceptual Design of an Unmanned Aerial Vehicle for Mars Exploration,” European Journal of Engineering and Technology Research, vol. 6, no. 5, pp. 111–117, Aug. 2021, doi: https://doi.org/10.24018/ejeng.2021.6.5.2528.
[3] K. FUJITA, R. LUONG, H. NAGAI, and K. ASAI, “Conceptual Design of Mars Airplane,” TRANSACTIONS OF THE JAPAN SOCIETY FOR AERONAUTICAL AND SPACE SCIENCES, AEROSPACE TECHNOLOGY JAPAN, vol. 10, no. ists28, pp. Te_5–Te_10, 2012, doi: https://doi.org/10.2322/tastj.10.te_5.
[4] Dodi DeAnne Walker, “Preliminary Design, Flight Simulation, and Task Evaluation of a Mars Airplane,” TRACE: Tennessee Research and Creative Exchange, 2024. https://trace.tennessee.edu/utk_gradthes/496/ (accessed Sep. 02, 2024).
[5] H. D. Kim, “Distributed Propulsion Vehicles,” Nasa.gov, Sep. 2010, doi: https://doi.org/100036222/downloads/20100036222.
[6] J. L. Felder, G. V. Brown, H. DaeKim, and J. Chu, “Turboelectric Distributed Propulsion in a Hybrid Wing Body Aircraft,” Sep. 2011.
[7] L. Leifsson, A. Ko, W. H. Mason, J. A. Schetz, B. Grossman, and R. T. Haftka, “Multidisciplinary design optimization of blended-wing-body transport aircraft with distributed propulsion,” Aerospace Science and Technology, vol. 25, no. 1, pp. 16–28, Mar. 2013, doi: https://doi.org/10.1016/j.ast.2011.12.004.
[8] J. Felder, H. Kim, and G. Brown, “Turboelectric Distributed Propulsion Engine Cycle Analysis for Hybrid-Wing-Body Aircraft,” 47th AIAA Aerospace Sciences Meeting including The New Horizons Forum and Aerospace Exposition, Jan. 2009, doi: https://doi.org/10.2514/6.2009-1132.
[9] H. D. Kim, J. L. Felder, M. T. Tong, and M. Armstrong, “Revolutionary Aeropropulsion Concept for Sustainable Aviation: Turboelectric Distributed Propulsion,” ntrs.nasa.gov, Sep. 09, 2013. https://ntrs.nasa.gov/citations/20140002510
[10] Z. Lyu and J. Martins, “Optimization of Area Navigation Arrival Routes for Cumulative Noise Exposure | Journal of Aircraft,” Journal of Aircraft, 2014, doi: https://doi.org/10.2514/ja.2014.51.issue-5;page:string:Article.
[11] M. Brown and R. Vos, “Conceptual Design and Evaluation of Blended-Wing Body Aircraft | AIAA SciTech Forum,” AIAA SciTech Forum, 2018, doi: https://doi.org/10.2514/MASM18;page:string:Article.
[12] C. Humphreys-Jennings, I. Lappas, and and D. M. Sovar, “Conceptual Design, Flying, and Handling Qualities Assessment of a Blended Wing Body (BWB) Aircraft by Using an Engineering Flight Simulator,” Aerospace, vol. 7, no. 5, p. 51, Apr. 2020, doi: https://doi.org/10.3390/aerospace7050051.
[13] A. Dorsey and A. Uranga, “Design Space Exploration of Blended Wing Bodies | AIAA AVIATION Forum,” AIAA AVIATION Forum, 2021, doi: https://doi.org/10.2514/MAVIAT21;article:article:10.2514/6.2021-2422;website:website:aiaa-site;wgroup:string:AIAA.
[14] N. Qin, A. Vavalle, and A. Le Moigne, “Spanwise Lift Distribution for Blended Wing Body Aircraft.,” Journal of Aircraft, vol. 42, no. 2, pp. 356–365, Mar. 2005, doi: https://doi.org/10.2514/1.4229.
[15] T. Desert, H. Bézard , J.-M. Moschetta, and T. Jardin, “Aerodynamic design of a Martian micro air vehicle,” HAL (Le Centre pour la Communication Scientifique Directe), Jul. 2019.
[16] H. HIDAKA and M. OKAMOTO, “An Experimental Study of Triangular Airfoils for Mars Airplane,” TRANSACTIONS OF THE JAPAN SOCIETY FOR AERONAUTICAL AND SPACE SCIENCES AEROSPACE TECHNOLOGY JAPAN, vol. 12, no. ists29, pp. Pk_21–Pk_27, Jan. 2014, doi: https://doi.org/10.2322/tastj.12.pk_21.
[17] A. Oyama and K. Fujii, “A Study on Airfoil Design for Future Mars Airplane,” 44th AIAA Aerospace Sciences Meeting and Exhibit, Jan. 2006, doi: https://doi.org/10.2514/6.2006-1484.
[18] S. Rajarajan, P. Surya, M. Karthikeyan, P. Manikandan, and K. Lokeshkumar, "Numerical study of unconventional airfoils at low Reynolds number for the application of Mars flight," 2021. International Journal of Applied Engineering Research, 16(5), 362-371. https://doi.org/10.13140/RG.2.2.33666.20163
[19] O. Șugar-Gabor and A. Koreanschi, “Design of Supercritical Low-Reynolds-Number Airfoils for Fixed-Wing Flight on Mars,” Journal of Aerospace Engineering, vol. 33, no. 5, p. 04020052, Sep. 2020, doi: https://doi.org/10.1061/(asce)as.1943-5525.0001166.
[20] D. P. Raymer, Aircraft Design : A Conceptual Approach. Washington, D.C, 1992.